Nigerian Research Journal of Chemical Sciences **(ISSN: 2682-6054)**
Volume 11, Issue 2, 2023

Synthesis and Characterization of a Nano Copper Based-Urea-Hydroxyapatite-Potassium (Cu-NPKnp) Composite: Towards a Multifunctional Cu-NPKnp for Improved Crop Nutrient and Green Environment, Part 1

[1]Kolawole Aremu Erubami-Abolade, [*1]Oluwasayo Kehinde Moyib,
[1]Oluwakemi Oluwabunmi Banjoko, [1]Oyesolape Basirat Akinsipo and [1,2]Saliu Alao Amolegbe

[1]Department of Chemical Sciences, Tai Solarin University of Education, Ijagun, Ogun State, Nigeria
[2]Department of Chemistry, Federal University of Agriculture, Abeokuta, Ogun State, Nigeria
*Corresponding Author moyibok@tasued.edu.ng

ABSTRACT

Nanomaterials have gained tremendous attention due to their morphology and appealing characteristics for applications in various fields including agricultural system and green environment. This research work designed a Cu-NPKnp composite from direct combination reaction of nanoparticles of copper oxide (CuOnp), urea-modified hydroxyapatite (U-HAnp) and potassium (Knp). The synthesized Cu-NPKnp composite was characterized using Ultraviolet-Visible (UV-Vis) spectroscopy, Fourier transform-infrared (FTIR) spectroscopy, Energy dispersive X-ray (EDX), Scanning electron microscopy (SEM), Transmission electron microscopy (TEM), Powder X-ray diffraction (PXRD) and Differential light scanning (DLS). FTIR analyses showed C=O, O-H. M-O, COO-M, and M(CO) functional groups and vibrations of N-H, C-O, O-H and PO_4^{2-}. EDX revealed main minerals as C, O, P, K, Ca, and Cu and with adsorption of O, C, K, and Cl from precursor's materials. UV-Vis showed several chemical modifications with $\pi \rightarrow \pi^*$ and $n \rightarrow \pi *$ transitions and its photosensitivity. PXRD showed signatures for CuOnp, Knp, U, HA, U-HA with unassigned signatures predicted as its unique identity. Combined SEM, TEM, and DLS revealed Cu-NPKnp as a black monoclinic crystal with embedded white U-HAnp and an average size of 14.0 nm. The synthesized functional material of Cu-NPKnp is nutrient- enriched and with possible adsorbent potential for agriculture and green environment applications.

Keywords: Copper oxide nanoparticle, Nitrogen, Phosphorus, Potassium nanoparticle, Cu-NPKnp composite, urea-hydroxyapatite nanoparticle

INTRODUCTION

The adventure into nanomaterials is a huge breakthrough with array of opportunities in the multiple fields such as optical, conductors, energy, medicine, pharmaceuticals, electronics, and agriculture. Nanomaterials and nanoparticles are general description of materials with dimension size between 1 and 100 nm, possess large surface area to volume ratio and various shape morphologies. Their seamless architectural design combined with their inherent and extrinsic chemical compositions give them distinctive properties for diverse applications. Examples of their various applications include biosensors and diagnostics, medical implants, skin tissue healing, electronic skin, bone repair, tooth replacement, electronic displays and touch screen, information displays, light emission diodes (LEDs), solar cells, optoelectronics, large format cheap microelectronics, human-machine interfaces, flexible devices, energy storage devices, clothes, packaging materials, cosmetics, smart fertilizer, catalysts, conductors, batteries, wastewater treatment, and adsorbents [1-14].

Transition elements and their oxides have proven to be good sources of nanoparticles. Copper oxide nanoparticles (CuOnp) are good conductors of heat and electricity, catalyst for cross coupling reactions, antimicrobial activities. In addition, CuOnp is photosensitive, optical transparent and can interact with other materials with less modification [14-21]. Copper nanoparticle has been reported as an excellent nanometal for rapid absorption and slow release in some plants [19-23] and as such a good candidate as nanofertilizer. Nanometal fertilizers are obtained in green synthesis using diverse biological materials as reducing and capping agents and hence, promoting green environment.

With the vast information on nanomaterials and their applications, there is continuous research into their properties for novel applications. Formulation of hybrid nanomaterials with multifunctional roles is being explored. Hybrid nanofertilizers incorporating more than one nanoparticle are recently reported to have better efficiency than single nanofertilizer. Hybrid fertilizers are composed of two or three nanoparcticles. Urea hydroxyapatite is a common nano hybrid that find many applications as smart N and P nutrient in agriculture, surface material, Ca and P in dentistry and orthopedic [6, 24-26]. There are reports of adding nanometal into biomass wastes as fertilizer for plant propagation [1, 11]. Also, a complex of CuOnp and ZnOnp was embedded on alginate for dual functions as soil conditioner and plant nutrient releaser [27].

Ahmed, Kabir and Xiong [2] formulated a dual-functional silver nanoparticle as a colorimetric Sensor for Hg^{2+}/Pb^{2+} and an efficient catalyst for degradation of methyl red.

Morphology and chemical attributes of the hybrid nanostructures are key factors for a multifunctional composite. Consequently, a multifunctional nanomaterial perhaps, requires more than two components to harness its full potentials. Therefore, the present research study designed a nanocomposite with four nanoparticles of urea, hydroxyapatite, potassium and copper oxide (Cu-NPKnp) that could be further explored for multiple functionalities in agricultural systems and environmental applications.

MATERIALS AND METHODS

All chemical reagents used are of analytical standard and were purchased from a local vendor. All wet chemical experiments were carried out in the Department of Chemical Sciences Laboratory, Tai Solarin University of Education, Ijagun, Ijebu-Ode, Nigeria. Characterization (microscopic and spectroscopic analyses) were carried out at University of Cape Town, South Africa and at Federal University of Agriculture (FUNAAB), Abeokuta. Modified methods were adopted for synthesis of nanohybrid U-HA, Knp and CuOnp as precursors in separate reactions and composited as nanohybrid Cu-NPKnp composite.

Synthesis of hybrid urea-modified hydroxyapatite nanoparticles (U-HAnp)

Tarafder et al. [26] method was adopted for synthesis of nano U-HAnp based on two-steps in situ chemical approach as source of N and P nutrients (Eqn. 1, 2).

$$\underset{\text{phosphoric acid}}{6H_3PO_4} + \underset{\text{calcium hydroxide}}{10Ca(OH)_2} \rightarrow \underset{\text{hydroxyapatite}}{10Ca(PO_4)6\,(OH)_2} + \underset{\text{water}}{18H_2O} \quad \text{.....Eqn. 1}$$

$$\underset{\text{trisodium citrate}}{Na_3C_6H_5O_7} + \underset{\text{bulk urea}}{3CH_4N_2O} \rightarrow \underset{\text{citric acid}}{C_6H_8O_7} + \underset{\text{nanourea}}{H_2N\,CO\,NH_2np} + \underset{\text{sodium hydrogen nitrite}}{3NaHNO_2} \quad \text{.....Eqn. 2}$$

Copper oxide nanoparticles (CuOnp)

The synthesis of CuOnp followed Ekanaye and Godakumbura [27] but copper chloride was used instead according to Eqn. 3. Exactly 1.0 M NaOH solution was added dropwise into 0.5 M $CuCl_2$ solution under constant stirring. The brown precipitate of $Cu(OH)_{2(s)}$ formed was washed

with dil. H_2O and centrifuged, three consecutive times. The precipitate was finally calcined at 350 °C for 2 h in air.

$$2NaOH + CuCl_2 \rightarrow CuOnp + 2NaCl + H_2O \quad \text{..... Eqn. 3}$$

sodium hydroxide *copper chloride* *nanocopper* *sodium chloride* *water*

Green synthesis of nanopotassium (Knp)

Biogenic wet process was adopted for synthesis of Knps using avocado (*Persea americana*) leaves as both a reducing and capping agent due to its rich phytochemicals, high fibre and biomolecules contents [28]. Fresh and healthy leaves sample of *P. americana* was pulverized using mortar. Then, 10 g pulverized leaves were mixed with 100 ml distilled water and agitated at pH 6.0, 60 °C and 24 h. Thereafter, 10 ml of aqueous extract of *P. americana* was mixed with 40 ml of 10 mM KCl and heated at 60 °C for 30 min. There was a colour change from pale yellow to brick red, indicating generation of Knp. Finally, the Knp mixture was centrifuged at 11200 rpm for 10 min, washed with sterile distilled water, transferred to a freeze dryer to obtain solid particulate powder and kept at normal room temperature for further use.

Synthesis of nano Cu-urea-modified-hydroxyapatite-potassium (Cu-NPKnp) composite

Three grams (3 g) nanohybrid U-HAnp, 3 g Knp, 1 g CuOnp, 10 ml 1.5 % sodium alginate, 5 ml 3 % $CaCl_2$ were added together in a 250 ml beaker and made up to 100 ml with dil. H_2O. The mixture was incubated at 4 ^oC overnight, air dried at room temperature for 24 h and stored in an air-tight container to avoid absorption of atmospheric moisture.

Physical and chemical characterization of synthesized of Cu-NPKnp composite

Various microscopic and spectroscopic methods were employed to reveal the morphological nature and chemical composition of the synthesized Cu-NPKnp composite.

Morphological structure and properties

Surface morphology and Nanostructure of Cu-NPKnp were observed using a Scanning Electron Microscope (FEI Technal 20) equipped with a Lab 6 emitter operating at 200 kv and fitted with a Gatan Tridem GIF 2K byb 2K CCD camera). The sample was directly dispersed on a carbon conductive tape and sputter-coated with 5 nm of gold using a quorum-Q150R Plus E sputter coater.

It was then placed on a charge reduction sample holder and introduced into the column of the SEM machine and viewed with a camera, then recorded for 20 and 50 nm magnifications. Also, transmission electron microscope (TEM) of Cu-NPKnp was used to observe its polymeric morphology using a carbon coated copper grid (300 mesh). The sample containing grids were dried for 24 h at room temperature prior to observation. Both imaging and selected area diffraction patterns were recorded. The phase composition and crystallinity were studied by powder X-Ray diffraction analysis (Bruker D8 Focus Empyrean diffractometer) using Cu Kα radiation (λ = 1.5418Å) source operated under a tension of 45 kV and tube current of 40 mA to generate the X-ray. The peaks obtained were matched with the minerals phases from the Powder Diffraction File.

Chemical components

The elemental composition of Cu-NPKnp was obtained using Energy Dispersive X-ray (EDX) while functional groups involving in interaction of Cu-NPKnp composite were obtained with Fourier transform infrared (FT-IR) spectra (Agilent Technology Cary 630 FTIR). All FTIR spectra were obtained in transmittance mode at 8 cm^{-1} resolutions over the spectral scan range of 4000 - 500 cm^{-1}. Ultraviolet visible (UV) spectra of Cu-NPKnp were obtained using UV-Vis spectrometer in absorption mode (DR6000^{TM} USA) at 5 cm^{-1} revolutions over the spectra wavelengths range of 200-800 nm.

RESULTS AND DISCUSSION

Surface morphology and structure of Cu-NPKnp composite

SEM at 20.0 nm magnification revealed the surface morphology of Cu-NPKnp as homogeneous crystalline nanobeads aggregated together with distinct barriers between white and black crystals while increasing the magnification to 50.0 showed a black crystal of Cu-NPKnp embedded in self-assembly white crystals of U-HAnp with slightly varying shapes and sizes as observed visually (Fig. 1a, b). Further analysis with TEM showed the nanobeads are monodispersed crystals and aggregated according to their crystalline structures and sizes in phases similar to SEM (Figure 1c, d). Nanobeads size ranged between 10.093 and 19.797 nm with an average of 14.154 nm (SD, 3.38), as determined by dynamic light scattering (DLS) technique based on the Brownian motion of dispersed particles using Image J App**.** Hence, the crystals aggregate according to their sizes, structures and compositions.

Kottegoda et al. [25] reported nanoparticle U-HA as rod-like and hexagonal structure but varying shapes with some irregularities are obtained at present study, which may be functions of preparation, proportion of reactant and process, source and final composition. Nevertheless, the monocrystalline structure of Cu-NPKnp composite of irregular and varying shapes obtained at present is considered monoclinic in nature and is in order with most reports on crystals. Scientists have reported diverse nanostructures that could be poly or mono crystals aggregated or closely packed due to agglomeration into diverse shapes of rod, spherical, hexagonal, rhombic, fibrous, hexagonal, cubic etc. [6, 24-27, 29, 30-34].

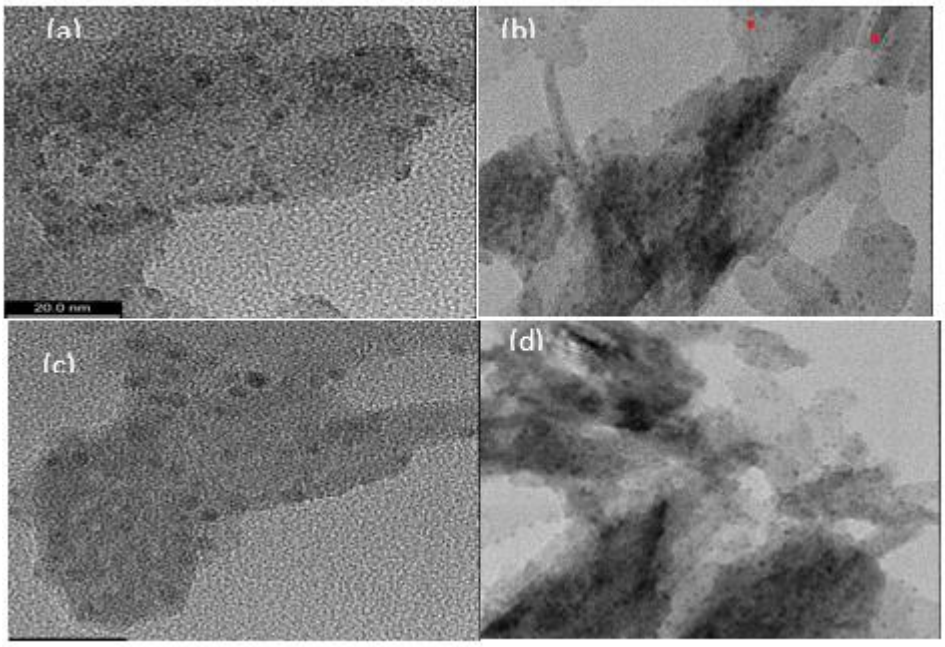

Figure 1. The surface morphology and nanostructure of Cu-NPKnp as revealed be SEM and TEM. a) SEM structure at 20.0 nm magnification, b) SEM structure at 50 nm magnification, c) TEM structure at 20. 0 nm and d) TEM structure at 50.0 nm. Both SEM and TEM are in conformity revealing a monocrystaline nanobeads packed together with distinct phases between hybrid U-NH-Knp and CuOnp.

Powder X-ray diffraction

The Powder XRD was conducted for depicting its crystalline structure which was confirmed from its well defined peak heights. The Powder XRD reveals monoclinic nature of Cu-NPKnp composite without altering the structure of self-assembled U-HAnp, and also shows corresponding

reflection plane structures similar to the referenced standard of copper nano powder. The PXRD spectra for U-AHnp in Fig. 2a displays peaks: 110, 200, 220 at different 2Θ degrees, correspond to reflection plane structure of rod-like and hexagonal for hybrid U-HAnp [24-26, 31]. Also, Peak 21.4 observed at 2Θ corresponds to reflection plane structure 200 for U [25), which could be considered as urea bulk peak before disintegrated and bonded with HA and its strong interaction with HA shift the peaks. Furthermore, the PXRD provided deeper overview into the observed phase and crystalline structure of Cu-NPKnp.

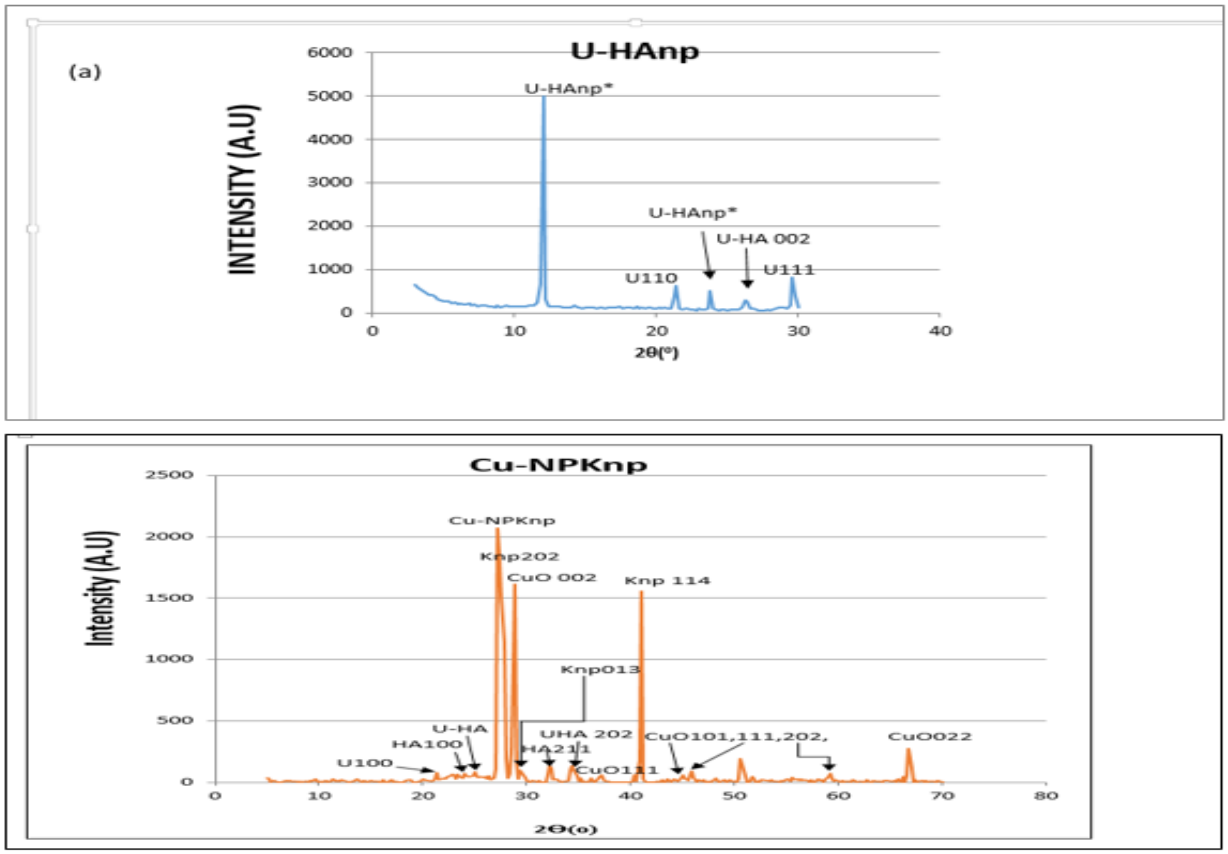

Figure 2: PXRD Patterns of a) hybrid U-HAnp, b) Cu-NPKnp composite. The PXRD reveals monoclinic nature of Cu-NPKnp without altering the structure of self-assembled U-HAnp, and also shows corresponding reflection plane structures for U-HAnp, CuOnp, Knp and Urea.

FTIR spectroscopy of U-HAnp and Cu-NPKnp

Fig. 3a shows FTIR spectrum with more than five spectra for U-HAnp, which signifies its complex nature. There are bands ranging between 3200 and 3550 cm^{-1}, suggestive of H bonding in hydrate

(H_2O), hydroxyl (OH), amino (NH_2) and or ammonium ion ($NH4^+$) [35]. The presence of NH stretch of primary amine (NH_2) of urea ranging across 3400-3500 cm^{-1} is supported with a NH bend at ≈1602 cm^{-1} and C-N stretch at 1065 cm^{-1} for a primary amine (NH_2). There are some spectra for C=O peak at ≈1630 cm^{-1} for urea amide and ketone at 1713 cm^{-1} of which high intensity of transmitter within 1600-1620 cm^{-1} range didn't allow distinct peaks between the observed C=O group and NH bend. These peaks are indicative of urea bonding to HA in hydrogen and nitrogen environment to form U-HAnp [24-26, 35-36]. The presence of spectra at frequencies of 1630-1600 cm^{-1}, 1200-1000 cm^{-1} confirms OH groups with a C-O stretch for primary alcohol at 1070 cm^{-1} (arrows not shown). Co-appearance of OH and N-H stretches are expected, because both appear at same wavenumber region [35]. The OH is resolved as H bonded OH stretch, dimeric OH---OH of urea to HA, and OH vibration of free hydroxyl group in U-HAnp. Peaks ranging 1100-1000 cm^{-1} depicts phosphate ions but reflected as a shift spectrum at 1170cm^{-1} due to P-O stretching in HA [24-26, 35-36].

Figure 3b displays spectra with more than five absorption bands for Cu-NPKnp composite, indicative of complex crystalline inorganic-organic salt with some broad bands above 3000 cm^{-1} showing presence of H bonding hydroxyl, exhibiting hydrates, alcohol, amine and or ammonium within 3200-3650 cm^{-1} [35]. A band of non-bonded H hydroxyl of alginic acid is observed at frequency 3602 cm^{-1} followed by H bonded OH stretch of HA hydroxyl at 3508 cm^{-1} and NH_2 stretch of urea at 3392 cm^{-1} for U-HAnp in Cu-NPKnp composite. An H bonded polymeric OH of alginic at frequency 3265 cm^{-1} confirms its crosslinking of the precursors in the Cu-NPKnp composite with its terminal C-H stretch at 3035 cm^{-1}. Therefore, broad bands ranging 3300-3030 cm^{-1} signifies presence of alginic acid crosslinking in Cu-NPKnp composite as clearly shown in Fig. 3b [27, 37]. There are unsaturated and saturated C-H stretches at transmittance peaks of above and below wavenumber 3000 cm^{-1}, respectively, which could be ascribed to alginic acid and *P. Americana* extract used as capping agent (27, 36-37). Transition metal carbonyl, M(CO), is detected at peaks 1912 and 1816 cm^{-1} that pinpointed presence of CuOnp [27, 36]. Noteworthy, Cu-NPKnp composite and U-HAnp were observed in the range of 500−4000 cm^{-1} and therefore, not afford transmittance peaks at higher wavenumber above 500 cm^{-1}. In addition, in Fig. 3b, the high intensity in the transmittance peaks <1000 cm^{-1} of Cu-NPK didn't allow peaks at higher wavenumbers >1000 cm^{-1} to be clearly observed. Nonetheless, the expected interatomic vibrations

of Cu-NPKnp shows significant absorption peaks below 1000 cm^{-1} which signify presence of M-O bonds within 900-600 cm^{-1} and therefore, highest transmittance intensity at 639 cm^{-1} was resolved for CuOnp and is within the range 450-650 cm^{-1} earlier reported for CuOnp [27, 30-32, 35].

There is presence of C=O group ranging at 1660 cm-^{1} which is below 1700 cm-^{1}, indicative of conjugated C=O from an amide group of urea, which led to a shift to lower absorption at 1650 cm^{-1}. A metal-carboxylate, COO-M group of alginate crosslink is identified at 1613 cm^{-1} and an alkaline metal carboxylate (COO-K) stretch is observed at 1484 cm^{-1}, indicating interaction of carboxylate group on alginate with potassium [36-37]. Absorption bands associated with group frequency for C-N stretch for NH_2 of urea shifted to 1062 cm^{-1} and also, a shifted peak for PO_4^{2-} of HA are observed at range 1165 cm^{-1} [25, 35].

Multiple and combination bands observed at present FTIR spectrum of Cu-NPKnp composite denotes several interactions within the composite involving functional groups on Knp surface contributed by *P. Americana* capping, functional groups on alginate, U-HA with Knp and CuOnp [25-27. 30-32, 35-37]. Furthermore, the observed similarity in the appearance OH, NH, C=O, and PO_4^{2-} peaks in the same frequency between U-HAnp and Cu-NPKnp suggests an absorption effect that lend credence to the nanocomposite phase of Cu-NPKnp.

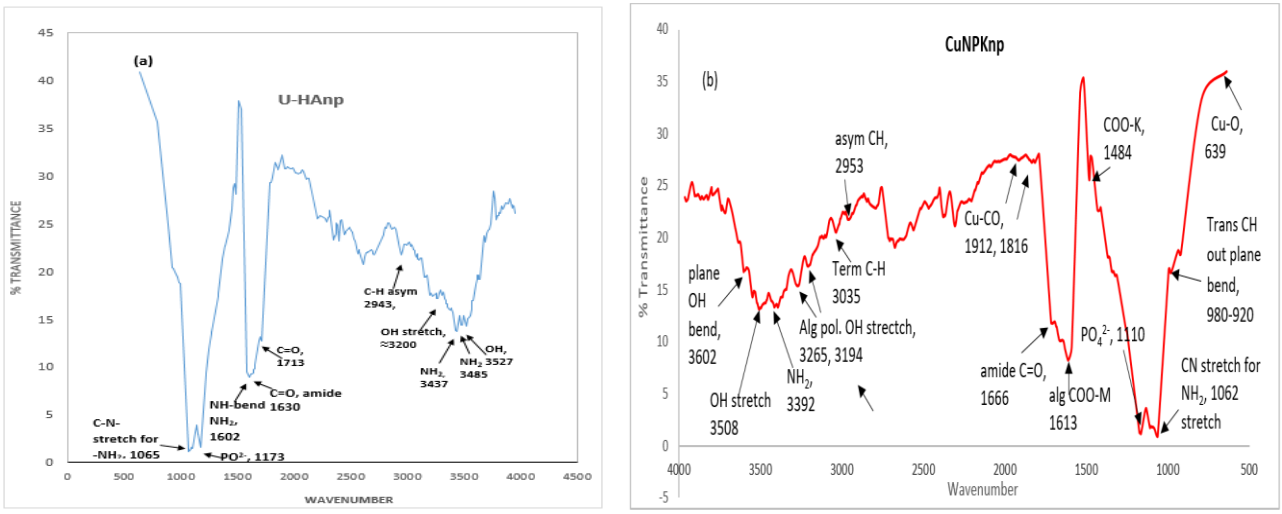

Fig. 3: FTIR spectrum of: (a) hybrid U-HAnp and (b) Cu-NPKnp composite, revealing H bonding between OH and NH in U-HAnp, C=O and C-N stretch for urea amide, PO_4^{2-} of HA, in both U-

HAnp and Cu-NPKnp; and Cu-CO, Cu-O bonds, COO-M and COO-K group of alginic acids in Cu-NPKnp composite are identified.

Energy dispersive X-ray (EDX) analysis of synthesized Cu-NPKnp

Figure 4 displays EDX spectra for the synthesized Cu-NPKnp composite revealing seven main elements, carbon (13.02%), oxygen (45.63%), sodium (3.55%), phosphorus (9.9%), potassium (5.41%), calcium (15.29%) and copper (5.89%) and traces of aluminum (0.85%) and chlorine (0.46%), perhaps from the precursors materials or environmental air during preparations. Absence of nitrogen in the EDX analysis may be due to overlapping of carbon and nitrogen emanating from its low efficiency in detecting low-Z atoms [38]. The presence of sodium on the surface of CuONp signifies its potential as a capping agent either from NaOH in the synthesis of CuOnp or sodium alginate for composition of Cu-NPKnp. There are also co-presence of Cl (5.33%), Ca (20.38%) on the surface of Knp (9%) that suggest them as capping molecules from *P. americana* extract and the large peak of carbon could be contributed by both *P. americana* and alginic acid.

Furthermore, the EDX spectra for the green synthesized K-NPs produced a strong signal at 3.5 keV, which confirms the existence of K and its organic components in its nano composition. The EDX results revealed the rich nutrient content of Cu-NPKnp composite, which signify its potential as a nutrient that could find uses in many applications including agriculture for soil/plant health, nutrient enrichment and high crop yield as previously reported for hybrid nanoparticles of its type [1, 6, 11-12, 23, 25-26].

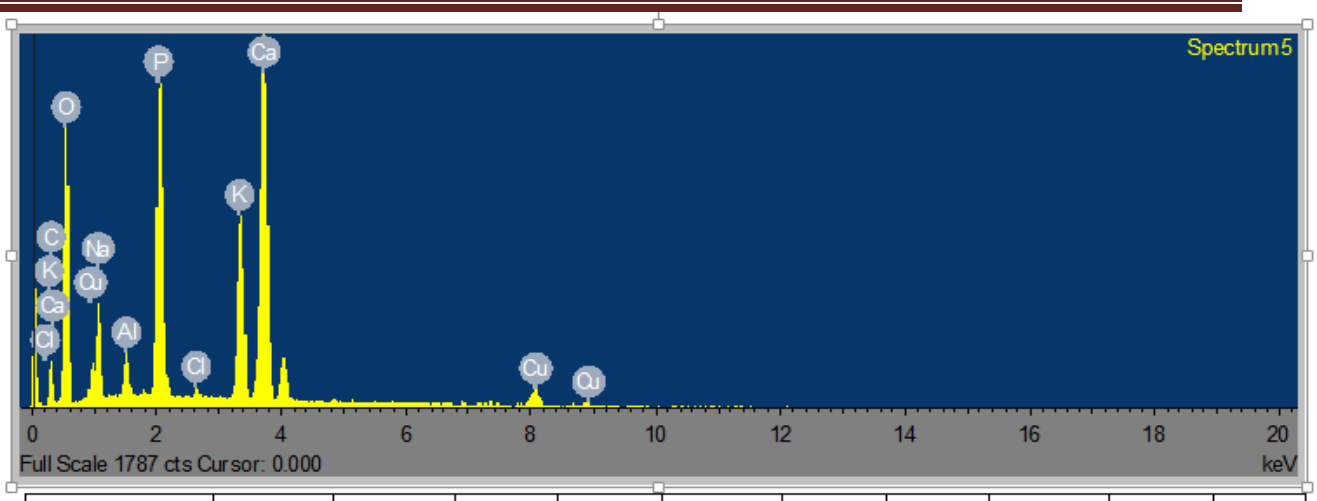

Element	C	O	Na	Al	P	Cl	K	Ca	Cu	
Mean%	13.02	45.63	3.55	0.85	9.9	0.46	5.41	15.29	5.89	100
SD	3.19	1.36	0.33	0.28	1.01	0.35	1.1	1.74	1.21	
Max.	18.48	47.89	4.06	1.15	11.08	1.08	6.89	17.46	7.04	
Min.	10.53	44.33	3.2	0.51	8.55	0.28	4.5	12.93	4.34	

Fig. 4: EDX spectra of Cu-NPK Fertilizer and the Tabular proportion of the elements.

UV-Visible spectroscopy of U-HAnp and Cu-NPKnp composite

According to Fig. 5a, the UV-VIS spectrum of Cu-NPKnp composite shows a strong characteristic absorption peak of 206.0 nm corresponding to high energy absorption at UV region indicating a $\pi \rightarrow \pi^*$ transition (C=O of CuOnp/urea). Also, a plasmon broad band is observed between 236.0 to 600.0 nm indicating the Cu-NPKnp composite is absorbing over a whole range of wavelengths; suggesting a whole range of energy jumps into visible region of n$\rightarrow \pi^*$ transitions requiring low energy, which could be lone pair from oxygen of CuOnp and nitrogen of U-HAnp. Therefore, there are rotations and vibrations in the molecule and are continually changing the energies of the orbitals revealing that the gaps between them are continually changing as well. Consequently, absorption takes place over a range of wavelengths and reasons for its black colour.

Same Fig 5b reveals a ƛmax 222.0 nm and broad base from 258.5 to 600.0 nm for Knp and decreased shift in both wavelength and absorbance were observed in the Cu-NPKnp composite, indicating both hypsochromic and hypochromic in nature, while it is bathchromic and

hyperchromic for CuOnp. Therefore, Cu-NPKnp composite is photosensitive in character which could be attributed to the presence of CuOnp, a transition nanoparticle. The present results reveal lots of chemical modifications during formation of Cu-NPKnp composite which is suggestive of its potential as adsorbent nanomaterial [3, 12]. This is evident in its chemical composition and with presence of adjunct molecules from precursors materials obtained in EDX analysis as added adsorptive properties. Hence, the numerous uses and applications of nanometals and nanomaterials are due to their functional surfaces that are good adsorbents that accelerate rate of chemical reactions, enhanced delivery of drugs and productivity [2, 8, 39]. Furthermore, CuOnp is noted for its electronic and optical properties and hence applications of its compounds in optical devices and photochemical devices [17, 20].

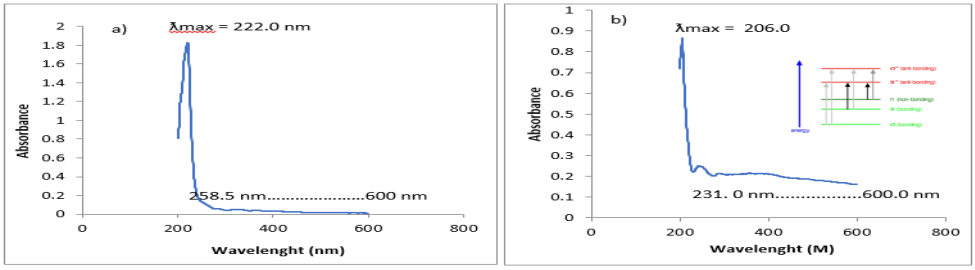

Figure 5: UV- VIS spectrum of: (a) Knp and (b) Cu-NPKnp composite. There are $\pi \rightarrow \pi^*$ transition of C=O and n$\rightarrow \pi^*$ transitions of lone pair from O and N atoms with vibrations taking place over a range of wavelengths.

CONCLUSIONS

The synthesized Cu-NPKnp composite was achieved through green and chemical sources as a black monoclinic crystal with an average size of 14.0 nm and signatures for nano CuOnp, Knp, U, HA, and U-HA. Nanosizing process involved C=O, OH, M-O, M(CO) and COO-M functional groups and vibration of N-H, C-O, CO-O^-, O-H and PO_4^{2-} with several chemical modifications of $\pi \rightarrow \pi^*$ and n$\rightarrow \pi *$ transitions. Cu-NPKnp is a photosensitive nano composite with enriched mineral constituents of C, P, K, Ca, O, and Cu with added surface molecules for enhancement of its functional roles. The current results present nano Cu-NPKnp composite as nutrient-enriched, and photo sensitive nanomaterial with possible adsorptive properties. Cu-NPKnp composite could find potentials in agricultural system for nutrient enhancement of soils and plants. Also, it could

be useful as a photosensitive material in electronics and optical photometric applications; and as an adsorbent for removal of unwanted or toxic elements in green environment preservation.

REFERENCES

1. Singh, P., Ghosh, D., Manyapu, V., Yadav, M. & Majumder, S. (2019). Synergistic impact of iron (iii) oxide nanoparticles and organic waste on growth and development of Solanum lycopersicum plants: New paradigm in nanobiofertilizer. *Plant Archives*, 19 (1), 339-344
2. Ahmed, F., Kabir, H. & Xiong, H. (2020). Dual colorimetric sensor for Hg^{2+}/Pb^{2+} and an efficient catalyst based on silver nanoparticles mediating by the root extract of *Bistorta amplexicaulis. Front. Chem. 8, 591958, 1-15. doi: 10.3389/fchem.2020.591958*
3. Attatsi, I.K., & Nsiah, F. (2020). Application of silver nanoparticles toward Co(II) and Pb(II) ions contaminant removal in groundwater. *Appl Water Sci* **10**, 152-165 https://doi.org/10.1007/s13201-020-01240-0
4. Ebrahim, S., Shokry, A., Khalil, M.M.A., Ibrahim, H. & Soliman, M. (2020). Polyaniline/Ag nanoparticles/grapheme oxide nanocomposite fluorescent sensor for recognition of chromium (VI) ions. *Scientific Reports*, 10, 13617, 1-11. https://doi.org/10.1038/s41598-020-70678-8.
5. Kianfar, E. (2020). Catalytic Properties of Nanomaterials and Factors Affecting it. Chp 4. Importance & Applications of Nanotechnology, Vol. 5, 22-25. *MedDocs Publishers, LLC e.book* http://meddocsonline.org/
6. Pohshna, C. & Mailapalli, D.R. (2022). Engineered Urea-doped Hydroxyapatite manomaterials as Nitrogen and Phosphorus fertilizers for Rice. *ACS Agric. Sci. Technol*., 2, 100-112
7. Ahlawat, J., Barroso, G.G., Asil, S.M., Alvarado, M., Armendariz, I., Bernal, J., Carabaza, X., Chavez, S, Cruz, P., Escalante, V., Estorga S. et al., (2021). Nanocarriers as potential drug delivery candidates for overcoming the blood−brain barrier: challenges and possibilities. *ACS Omega, xxx. 1-13* https://dx.doi.org/10.1021/acsomega.0c01592
8. El-Bahr, S.M. Elbakery, M., El-Gazzar, N., Amin, A.A., Al-Sultan, S., Alfattah, M.A., Shousha, S., Alhojaily, S., Shathele, M., Sabeq, I.I., & Hamouda, A.F. (2021). Biosynthesized iron oxide nanoparticles from *Petroselinum crispum* leaf extract mitigate

lead-acetate-induced anemia in male albino rats: hematological, biochemical and histopathological features. *Toxics*, 9, 123, 1-17. https:// doi.org/10.3390/toxics906012

9. Prodanov, M.F., Vashchenko, V.V. & Srivastava, A.K. (2021). Progress toward blue-emitting (460–475 nm). Nanomaterials in display applications. *Nanophotonics*, 10(7), 1801-1836.
10. Akhtar, N., Ilyas, N., Meraj, T.A., Pour-Aboughadareh, A., Sayyed, R.Z., Mashwani, Z.-u.-R., & Poczai, P. (2022). Improvement of plant responses by Nanobiofertilizer: A dtep towards sustainable sgriculture. *Nanomaterials*, 12, 965-987. https:// doi.org/10.3390/nano12060965
11. Abdel-Hakim, S.G, Shehata, A.S.A., Moghannem, S.A., Qadri, M., El-Ghany, M.F.A., Abdeldaym, E.A. & Darwish, O.S. (2023). Nanoparticulate fertilizers increase nutrient absorption efficiency and agro-physiological properties of lettuce plant. *Agronomy*, 13, 691-710. https://doi.org/10.3390/ agronomy13030691
12. Gangwara, J., Singh, A.P., Marimuthuc, N. & Sebastian. J.K. (2023). Environmentally sustainable zinc oxide nanoparticles for improved hazardous textile dye removal from water bodies. *AQUA-Water Infrastructure, Ecosystems and Society*, 72(7), 1198, 1-15, doi: 10.2166/aqua.2023.023
13. Hasan, Z. Zubair, M.O. & Hassan, T. (2023). Synthesis and characterization of cellulose nanomaterials from waste newspapers. *Mater. Proc.*, 14, 74. 1-8. https://doi.org/10.3390/
14. Jayeoye, T.J., Supachettapun, C., & Muangsin, N. (2023). Toxic Ag^{+} detection based on Au@ Ag core shell nanostructure formation using Tannic acid assisted synthesis of Pullulan stabilized gold nanoparticles *Scientific Reports*, 13, 1844, 1-15. https://doi.org/10.1038/s41598-023-27406-9
15. Manasrah, A. D. et al. (2018) Surface modification of carbon nanotubes with copper oxide nanoparticles for heat transfer enhancement of nanofluids. *RSC Adv.*, 8,1791-1802.
16. Kanwar, R., Bhar, R. & Mehta, S.K. (2018). Designed meso-macroporous silica framework impregnated with copper oxide nanoparticles for enhanced catalytic performance. *Chem Cat Chem*., 10, 2087-2095

17. Chaudhary, S., Rohilla, D., Umar, A., Kaur, N. & Shanavas, A. (2019). Synthesis and characterizations of luminescent copper oxide nanoparticles: toxicological profiling and sensing applications. *Ceram. Int.*, 45. 15025-15035
18. Hassan, S.E.D., Fouda, A., Radwan, A.A., Salem, S.S., Barghoth, M.G., Awad, M.A., Abdo, A.M., El-Gamal, M.S. (2019). Endophytic actinomycetes streptomyces spp mediated biosynthesis of copper oxide nanoparticles as a promising tool for biotechnological applications. *J. Biol. Inorg. Chem.*, 24 (3), 377-393
19. Keabadile, O.P., Aremu, A.O., Elugoke. S.E. & Omolola E.F. (2020). Green and traditional synthesis of copper oxide nanoparticles-comparative study. *Nanomaterials*, 10, 2502-2521. doi:10.3390/nano10122502 www.mdpi.com/journal/nanomaterials.
20. Dhineshbabu, V., Rajendran, N., Nithyavathy, R., & Vetumperuma, l. (2016). Study of structural and optical properties of cupric oxide nanoparticles. *Appl Nanosci.*, 6, 933-939
21. Renuga, D., Sundaru, J.J. & Athithan, A.S. (2022). Green Synthesis and Characterization of metal oxide nanoparticles using *Nelumbo nucifera* flower and its antimicrobial activities. *IJIRSET*, 11(1), 519-526
22. López-Vargaz, E.R., Ortiz, H.O., Cadenas-Pliego, G., Romenus, K.D-A., Fuente, M.C.D-L., Mendoza, A.B., & Maldonado, A.J. (2018). Foliar application of copper nanoparticles increases the fruit quality and the content of bioactive compounds in tomatoes. *Appl.Sc.*, 8(7), 1020-1028
23. Abbasifar, A., Shahrabadi, F., ValizadehKaji, B. (2020). Effects of green synthesized zinc and copper nano-fertilizers on the morphological and biochemical attributes of basil plant. J. Plant Nutr. 43 (8), 1104-1118.
24. Chandrasekar, A., Sagadevan, S. & Dakshnamoorthy, A. (2013). Synthesis and characterization of nano-hydroxyapatite (n-HAP) using the wet chemical technique *IJPS,* 8(32),1639-1645
25. Kottegoda, N., Sandaruwan, C., Priyadarshana, G., Siriwardhana, A., Rathnayake, U.A., Arachchige, D.M.B., Kumarasinghe, A.R., Dahanayake, D., Karunaratne, V. & Amaratunga, G.A.J. (2017). Urea-Hydroxyapatite Nanohybrids for Slow Release of Nitrogen. *ACS Nano*, 11, 1214−1221. DOI: 10.1021/acsnano.6b07781

26. Tarafder, C., Daizy, M., Alam, M.M., Ali, M.R., Islam, M.J., Islam, R., Ahommed, M.S., Aly, M.A.S., & Khan, M.Z.H. (2020). Formulation of a Hybrid Nanofertilizer for Slow and Sustainable Release of Micronutrients. *ACS Omega*, 5, 23960−23966
27. Ekanayake, A. & Godakumbura, P.I. (2021). Synthesis of a dual-functional nanofertilizer by embedding ZnO and CuO nanoparticles on an alginate-aased hydrogel. *ACS Omega*., 6, 26262−26272
28. Bhuyan, D.J., Alsherbiny, M.A., Perera, S., Low, M., Basu, A., Devi, O.A., Barooah, M.S., Li, C.G., & Papoutsis, K. (2019). The odyssey of bioactive compounds in avocado (*persea americana*) and their health benefits. *Antioxidants*, *8*(10), 426. https://doi.org/10.3390/antiox8100426
29. Sanchez, C., Boissiere, C., Cassaignon, S., Chaneac, C., Durupthy, O., Faustini, M., Grosso, D., Laberty-Robert, C., Nicole, L., Portehault, D., et al. (2014). Molecular engineering of functional inorganic and hybrid materials. *Chem. Mater*., 26, 221−238.
30. Siddiqui, H., Parra, M.R., Qureshi, M.S., Malik, M.M., & Haque, F.Z. (2018). 1Studies of structural, optical, and electrical properties associated with defects in sodium-doped copper oxide (CuO/Na) nanostructures. *J Mater Sci Ceramics* https://doi.org/10.1007/s10853-018-2179-6
31. Merkys, A., Vaitkus, A., Grybauskasm A., Konovalovas, A., Quiros, M., & Grazulis, S. (2023). Graph isomorphism-based algorithm for cross-checking chemical and crystallographic descriptions, *J Cheminformatics*, 15(25), http://doi:10.1186/S13321-23-00692-1
32. Khashan, K.S., Jabir, M.S., & Abdulameer, F.A. (2018). Preparation and characterization of copper oxide nanoparticles decorated carbon nanoparticles using laser ablation in liquid. *Journal of Physics: Conf. Series*, 1003**,** 012100, 1-7
33. Nido, P.J., Migo, V., Maguyon-Detras, M.C., & Alfafara, C. (2019). Process optimization potassium nanofertilizer production via ionotropic pre-gelation using alginate-chitosan carrier. *MATEC Web of Conferences*, 268, 05001, 1-5. https://doi.org/10.1051/matecconf/201926805001

34. Renuga, D., Jeyasundari, J., Athithan, A.S.S & Jacob, Y.B.A. (2020). Synthesis and characterization of copper oxide nanoparticles using *Brassica oleracea var. italic* extract for its antifungal application. *Mater. Res. Express.* 7, 04500, 1-6 https://doi.org/10.1088/2053-1591/ab7b9
35. Coates, J. (2000). Interpretation of Infrared Spectra: A Practical Approach. In R.A. Meyers (Ed.) Encyclopedia of Analytical Chemistry. pp 10815-10837. John Wiley & Sons Ltd, Chichester.
36. Nandiyanto, A.B.D., Oktiani, R., Ragadhita, R. (2019). How to Read and Interpret FTIR Spectroscope of Organic Material. *IJOST*, 4 (1), 91-118.
37. Corradini, E., DeMoura, M.R., Mattoso, L.H.C. (2010). A preliminary study of the incorporation of NPK fertilizer into chitosan nanoparticles. *eXPRESS Polymer Letters*, 4(8), 509-515.
38. Wolfgong, W.J. (2016). Chemical analysis techniques for failure analysis: Part 1, common instrumental methods, Chapter 14, Makhlouf, A.S.H. & Aliofkhazraei, M. (Eds). Handbook of Materials Failure Analysis with Case Studies from the Aerospace and Automotive Industries. Pp, 279-307. Elsevier.
39. Park, D.K., Lee, S.J., Lee, J.H., Choi, M.Y., & Han, S.W. (2010). Effect of polymeric stabilizers on the catalytic activity of Pt nanoparticles synthesized by laser ablation. *Chemical Physics Letters*. 2010, 484(6), 254-257.